Mayank V. Bendarkar, Dushhyanth Rajaram, Yu Cai, Simon Briceno, Dimitri N. Mavris. "Evaluating Optimal Paths for Aircraft Subsystem Electrification in Early Design", AIAA Aviation 2019 Forum (AIAA 2019-2802) https://doi.org/10.2514/6.2019-2802
https://arc.aiaa.org/doi/10.2514/6.2019-2802

Evaluating Optimal Paths for Aircraft Subsystem Electrification in Early Design

Mayank V. Bendarkar*, Dushhyanth Rajaram †, Yu Cai ‡,
Simon Briceno§ , and Dimitri N. Mavris¶
Aerospace Systems Design Laboratory, Georgia Institute of Technology, Atlanta, Georgia, 30332

The aerospace industry's push for More-Electric Aircraft (MEA) has motivated numerous studies to quantify and optimize the impact of subsystem electrification in early design phases. Past studies on multi-objective optimization of MEA show a clear benefit over conventional architectures when no constraints are placed on the number of subsystems electrified at once. In reality however, aircraft manufacturers are more likely to progressively electrify subsystems over multiple aircraft generations. While step-by-step electrification may lead to sub-optimal intermittent MEA architectures when compared with scenarios with no such imposition on number of subsystems electrified, little or no literature was found to address the optimal paths towards such electrification changes. The primary aim of this study is the creation of a mathematically defensible methodology that provides decision makers with the ability to analyze several paths for electrification of MEA subsystems while considering Pareto-optimality and other metrics based on objectives of interest in early design. It is hoped that decision makers will be able to understand the performance trade-offs between different electrification paths under different scenarios, constraints, and uncertainties. The resulting methodology is demonstrated on an exercise in the electrification of a Small Single Aisle aircraft.

Nomenclature

N = Total number of subsystem electrification options over baseline
$\mathbf{A}$ = An architecture defined by subsystem electrification choices
O_i = Set of Pareto Optimal architectures with maximum i ($i \leq N$) electrification changes over baseline

I. Introduction

Aircraft conceptual design involves computing parameters that define the vehicle through a weight breakdown, and geometric and propulsive scale given mission and point performance requirements. Conventional configurations rely heavily on historical data for their sizing, and rarely incorporate the effects of subsystems. Even when subsystems are considered, they are sized based on historical regressions due to maturity of data available [1–3]. The recent interest in more-electric architectures, where one or more subsystems may be partially or fully electrified, exists mainly because of the promise of potential improvements in fuel efficiency over technologically saturated conventional designs [4, 5]. However, scarcity in historical data for the more-electric architectures necessitates a first-principle physics based approach to estimate their sizing and performance effects in the conceptual aircraft design phase [6–9]. In order to quantify the impact of subsystem electrification in early design using first-principles, the Integrated Subsystem Sizing and Architecture Assessment Capability (ISSAAC) module was developed by Chakraborty [6, 10] and was improved upon by Cai et al. [11]. ISSAAC is an integral part of the current study and will be discussed in greater detail in Sec III.A.

In studies on integrated sizing and multi-objective optimization of aircraft with more-electric architectures by Rajaram et al. [12, 13], substantially electrified subsystems were found to dominate the Pareto frontier over conventional

*Senior Graduate Researcher, Daniel Guggenheim School of Aerospace Engineering, AIAA Student Member
†Senior Graduate Researcher, Daniel Guggenheim School of Aerospace Engineering, AIAA Student Member
‡Senior Graduate Researcher, Daniel Guggenheim School of Aerospace Engineering, AIAA Student Member
§Senior Research Engineer, Daniel Guggenheim School of Aerospace Engineering, AIAA Senior Member
¶S.P. Langley NIA Distinguished Regents Professor, Daniel Guggenheim School of Aerospace Engineering, AIAA Fellow

designs. Their study assumed that all subsystems could be electrified at once. As such, the decision to determine the number of subsystems that could be electrified at once was relinquished to the optimizer. Aircraft original equipment manufacturers and their suppliers have traditionally been cautious about introducing a novel technology on aircraft due to multiple important factors. First, there is inherent uncertainty and risk associated with maturation of a new technology to justify its incorporation on-board an aircraft. Second, aircraft manufacturers and suppliers only have enough resources to research and develop a couple of novel technologies at once. Hence, it is likely that any decision to electrify subsystems will be staggered into multiple steps with different subsystem(s) electrified gradually in successive generations of aircraft to reduce the risk associated with making multiple technological leaps at once. In other words, while literature is abound with finding optimal MEA architectures, there is very little focus on how to get there. In practice, realistic scenarios will involve a sequence of subsystem electrification changes, where the desire to remain optimal with respect to relevant design objectives may not always be fulfilled. Moreover, depending on how various objectives are weighted, several electrification paths may exist to reach the same final architecture. The decision of which path to take while maintaining optimality or remaining as optimal as possible motivates the need for this work.

Constraining the number of subsystems electrified will result in the so-called constrained Pareto optimal sets O_i (see Sec. II.A.5 for further details). The decision on which architecture to choose at any generational level (where $< N$ changes have already been made) becomes a multi-attribute decision making problem. The subsystem changes locked in at every generation while reaching the N^{th} change gives rise to the notion of the path of progressive subsystem changes. Different optimal paths may exist not only when considering multiple objectives (like MTOW, emissions, TOFL etc.) at each generational level, but also when weighing the multi-objective improvements of different generations uniquely. As such, many equally optimal (incomparable) paths (in the multi-objective setting) will result with i subsystem changes each. This set can then be leveraged by engineers to make better informed decisions. A method to provide this decision making capability is the primary goal and novel feature of this work. Additionally, some assumptions with regard to subsystem changes made by Rajaram et al. [13] to make the optimization problem tractable will be relaxed to consider a larger combinatorial space. However, the continuous aircraft level design variables will be fixed to manage the associated computational cost. The intent is to enable designers to make an unbiased assessment of sequential subsystem electrification choices, their benefits, and detriments.

The remainder of the paper is organized as follows – Section II gives an overview of the problem at hand, establishes notation that will be used for the rest of this paper, and formulates the hypotheses to be tested in this work. Section III gives a brief summary of Integrated Subsystem Sizing and Architecture Assessment Capability (ISSAAC), which is used in this work, followed by verifying the hypotheses, and defining the path optimality criteria. Sec IV discusses the results obtained along with a sensitivity study to quantify the impact of modeling uncertainty on the results. Section V concludes the present work and identifies future work.

II. Problem Formulation

In an effort to reduce the size of the combinatorial space, previous studies on subsystem architectures [7, 12] considered subsystem electrification bundles or packages using reasoning based on rules with regard to a natural electrification ordering due to technology maturation status. For instance, the predefined strategy for Actuation Function Packages (AFPs) included the Primary Flight Control Actuators (PFCA, that include elevators, ailerons, and rudder), Trimmable Horizontal Stabilizer Actuation (THSA), Spoiler Actuation (SPLA), leading and trailing edge High Lift Device Actuation (HLDA), Nose Wheel Steering System (NWSS), Landing Gear Actuation System (LGAS), Wheel Brake System (WBS), and Thrust Reverser Actuation System (TRAS). In this study however, it is assumed that all the subsystem components mentioned above can be electrified independently. There are two reasons to adopt this approach: 1) to mimic scenarios where all the allowable changes are equally mature technologically, 2) to demonstrate the method proposed in this work for cases where a significant combinatorial space of solutions exists. As such, the discrete options presented above are considered alongside the Wing Ice Protection System (WIPS), Cowl Ice Protection System (CIPS), and Environmental Control System (ECS) adding up to a total of eleven discrete options for electrification. An 11-digit architecture descriptor string (see Fig. 1) allows for a compact representation of the state of an electrified aircraft. For a fixed set of aircraft level continuous variables, the total number of possible More Electric subsystem combinations is a staggering 13,824. Since the primary aim of this paper is to provide a method that enables decision making when considering multiple progressive changes while maintaining optimality, the aircraft level continuous design variables are fixed. Next, some notation that enables a mathematically precise definition of the problem at hand is established.

Table 1 Matrix of Alternatives (MoA) for Subsystem Electrification

Subsystems	Options (Descriptor digit)	#
Thrust Rev. Act. Sys. (TRAS)	(0) Hydraulic, (1) Electric	2
Wheel Brake Sys. (WBS)	(0) Hydraulic, (1) Electric	2
Landing Gear Act. Sys. (LGAS)	(0) Hydraulic, (1) Electric	2
Nose Wheel Steer Sys. (NWSS)	(0) Hydraulic, (1) Electric	2
LE/TE High Lift Dev. Act. (HLDA)	(0) Hydraulic, (1) Electric	2
Spoiler Act. (SPLA)	(0) HA, (1) EHA, (2) EMA	3
Trim. Hor. Stabilizer Act. (THSA)	(0) Hydraulic, (1) Electric	2
Primary Flt. Cntrl. Surfs. (PFCA)	(0) HA, (1) H/EHA, (2) EHA, (3) EMA	4
Wing Ice Prot. Sys. (WIPS)	(0) P-Ev-AI, (2) E-RW-AI, (3) E-RW-DI	3
Cowl Ice Prot. Sys. (CIPS)	(0) P-Ev-AI, (2) E-Ev-AI, (3) E-RW-AI	3
Env. Ctrl. Sys. (ECS)	(0) Pneumatic, (1) Electric	2
	Total combinations: 13,824	

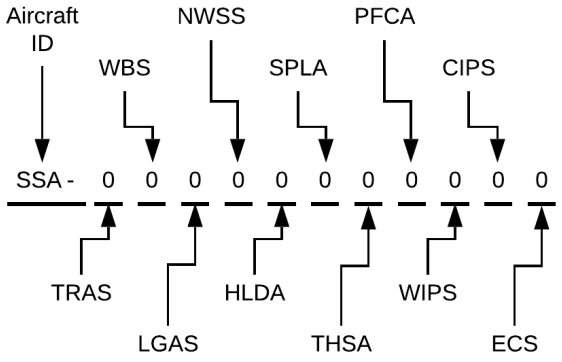

Fig. 1 Subsystem architecture descriptor. Refer to Table 1

A. Notation

1. Vehicle Baseline

The vehicle baseline architecture ($\mathbf{A_B}$) is defined as a fully conventional architecture with no subsystem electrified (from Table 1). This architecture is given by descriptor *SSA-00000000000*, and serves as an anchor point for all comparisons. The aircraft-level design variables for $\mathbf{A_B}$ are based on a Small Single-aisle Aircraft (SSA) given in Table 3 found in the Appendix. These aircraft level design variables are assumed constant for all the architectures that result after subsystem electrification.

2. Predecessor

An architecture $\mathbf{A_p}$ as given by its descriptor is a 'predecessor' of any architecture $\mathbf{A}$ if and only if it follows the following rules

1) $\mathbf{A_p} \neq \mathbf{A}$, and
2) $\mathbf{A_p}$ has certain subsystems common with $\mathbf{A}$, and
3) $\mathbf{A_p}$ has all other (uncommon) subsystems less electrified than $\mathbf{A}$. The following rules are used to determine if the

uncommon subsystems are less electrified*:

1) For TRAS, WBS, LGAS, NWSS, HLDA, THSA, WIPS, CIPS, and ECS the the corresponding descriptor has to be 0 (same as the baseline). Note for WIPS and CIPS, this means descriptor 2 is not considered as a predecessor of descriptor 3 because they are not comparable in terms of electrification.
2) For SPLA and PFCA, the descriptor in $\mathbf{A_p}$ must be numerically smaller than its corresponding value in $\mathbf{A}$.

3. Successor

A successor architecture, or merely 'successor' is the converse of a predecessor. If architecture $\mathbf{A_p}$ is a predecessor of $\mathbf{A}$, then by definition, architecture $\mathbf{A}$ is a successor of $\mathbf{A_p}$. The notation $\mathbf{A_s}$ will also be used to identify a successor of architecture $\mathbf{A}$.

It is important to note that certain architectures will remain incomparable by these definitions. The following examples can be used to illustrate this – *SSA-10000100000*, *SSA-01000000000*, *SSA-10000102000* are all predecessors of *SSA-11000003300*, while *SSA-00000003200* and *SSA-11000003300* are incomparable due to the WIPS of the former not being equal to zero.

4. Electrification Changes over Baseline

Number of subsystem electrification changes over baseline is defined as the number of subsystems that are electrified in a given architecture $\mathbf{A}$ when compared to the baseline. While computing this number, for the WIPS and CIPS subsystems, a descriptor change from 0 (baseline) to 2 or from 0 to 3 is considered as one change. For all other subsystems, the number of changes is simply the difference between the corresponding descriptor digit and the baseline value of 0. The total number of electrification changes over baseline for a given architecture $\mathbf{A}$ is then the sum of all individual subsystem changes. For example, *SSA-00000000320* has number of changes over baseline equal to two (WIPS and CIPS are counted as one change each), while *SSA-00000203000* has 5 subsystem electrification changes over baseline since for SPLA, descriptor $2 > 1 > 0$ in terms of electrification, while for PFCA, descriptor $3 > 2 > 1 > 0$ in terms of electrification.

5. Constrained Pareto Optimal Sets O_i

Rajaram et al. evaluated the unconstrained Pareto optimal set of architectures in a multi-objective optimization problem [13]. In the current study, the constrained Pareto optimal set O_i is defined as the set of Pareto optimal architectures that have at most $i \in \{1, 2, \ldots, 14\}$ subsystem electrification changes over baseline (refer Tab. 1). The unconstrained Pareto optimal set is denoted as O_N. Therefore, the set O_i can potentially include architectures having zero to i changes over the baseline.

6. Paths towards Subsystem Electrification

The definition of a path to subsystem electrification can now be established. Considering $\mathbf{A_B}$ as the source node, and a designated architecture $\mathbf{A_t}$ as the terminal node, a directed acyclic graph $\mathbf{G}$ can now be constructed between the two with the following rules (with architectures serving as nodes):

1) Every node in $\mathbf{G}$ (except $\mathbf{A_t}$) will be a predecessor of $\mathbf{A_t}$, and
2) Every edge in $\mathbf{G}$ will connect a predecessor architecture to its successor such that the difference in the number of subsystem electrification changes between the nodes connected by a single edge will be exactly equal to one

$\mathbf{G}$ can be described using an adjacency matrix where the rows and columns represent each predecessor of $\mathbf{A_t}$, with the (i, j)th entry equal to 1 if row $\mathbf{A_i}$ is a predecessor of column $\mathbf{A_j}$ and has exactly one fewer change compared to $\mathbf{A_j}$. The (i, j)th entry is zero otherwise. Thus, all sets of edges that connect $\mathbf{A_B}$ to $\mathbf{A_t}$ within $\mathbf{G}$ can be defined as valid paths towards subsystem electrification. At the same time, all valid paths will have edges that connect predecessors to their successors with exactly one additional electrification change in the subsystems.

Figure 2 shows an example directed acyclic graph $\mathbf{G}$ with a source node $\mathbf{A_B}$ and terminal node $\mathbf{A_t}$ with five intermediate nodes. All the missing elements of the adjacency matrix shown are zero. In this case, all possible paths between the source and terminal nodes can be elaborated. However, since we are dealing with a full-factorial DoE, we note that such graphs can contain thousands of nodes, making finding all possible paths between the baseline and architectures in O_N a computationally intractable problem for early aircraft design process.

*By this definition, the baseline $\mathbf{A_B}$ is a predecessor of all other architectures

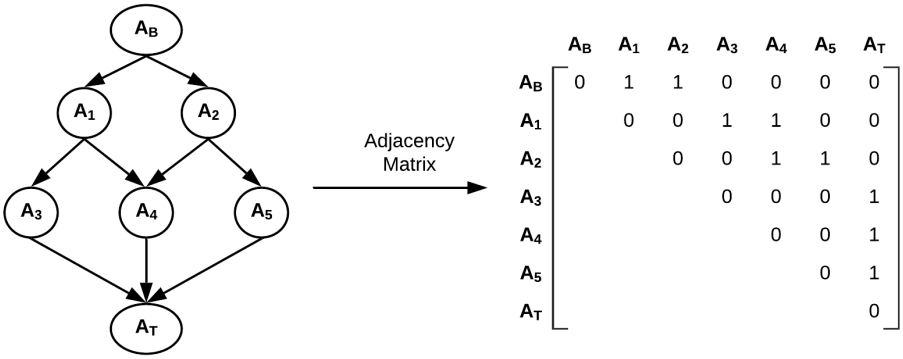

Fig. 2 Example adjacency matrix describing a directed acyclic graph

B. Need for Optimal Paths

With the notation now established, the following three hypotheses are examined to establish the need for determining optimal paths towards subsystem electrification:

1) Constrained Pareto optimal sets O_i ($i \in \{1, 2, \ldots, N-1\}$) are different from the unconstrained Pareto optimal set O_N
2) There exists at least one architecture $\mathbf{A} \in O_i$ such that at least one of its predecessors $\mathbf{A_p} \notin O_j$ ($0 < j < i \leq N$)
3) There exists at least one architecture $\mathbf{A} \in O_i$ ($i \in \{1, 2, \ldots, N-1\}$) such that all of its successors $\mathbf{A_s} \notin O_N$

The first hypothesis states that the non-dominated solutions obtained by subsystem electrification when constraints are placed on total number of subsystem changes over baseline will be different from the case where no such constraints are imposed. Rajaram et al. [13] showed a significant benefit of more-electric architectures when there are no constraints on number of changes over baseline. This paper will demonstrate how that changes under constraints.

The second hypothesis states that there will be some architectures $\mathbf{A} \in O_i$ such that not all one-change-at-a-time-paths leading from the baseline to those will be optimal – some paths will be such that their intermediate predecessors will not lie on the intermediate Pareto frontiers O_j ($j < i$). Thus, it claims that there will exist sub-optimal paths of reaching the Pareto optimal set of up to i changes over baseline ($O_i,\ i \in \{1, 2, \ldots, N\}$).

The third hypothesis states that there will exist certain architectures that will show up on the constrained Pareto frontiers O_i ($i \in \{1, 2, \ldots, N-1\}$), but any paths leading forward (in terms of successors) from these architectures will not reach the unconstrained Pareto frontier O_N. Thus, certain architectures might show promise when allowable number of subsystem changes is severely constrained, but will fail to maintain optimality when such constraints are relaxed. If aircraft conceptual designers decide to go down the path to reach these architectures, they can find themselves having to revert certain subsystem changes in order to maintain optimality, a proposition that can be very costly.

Taken together, these three hypotheses will seek to inform aircraft conceptual designers that merely knowing the optimal solutions to the unconstrained subsystem electrification problem is insufficient to make a decision regarding the optimal paths to get there. Verifying these hypotheses empirically will mean that not all paths within $\mathbf{G}$ will be optimal even though certain intermediate or final architectures in these paths lie on a Pareto front. Therefore, the importance to determine the optimal path towards subsystem electrification can be established.

III. Technical Approach

A. Integrated Subsystem Sizing and Architecture Assessment Capability (ISSAAC)

The ISSAAC environment, developed by Chakraborty [10] and used in this work, is briefly described in what follows for completeness. ISSAAC consists of seven modules, which themselves are tool agnostic in light of typical industry situations. However, tools that can collectively size the airframe for a particular mission, analyze the propulsion cycle for the power plant, and perform sizing and analysis of subsystems may be integrated to perform this work. For the present study, the Flight Optimization System (FLOPS), a legacy aircraft synthesis software developed by NASA [14], the Numerical Propulsion System Simulation (NPSS) providing engine cycle analysis capability [15], and a subsystem sizing and analysis module coded in MATLAB are used for the respective functionalities required. Details of the specific

governing equations modeling each of the subsystem components are omitted because they are not the primary focus of the current work. While methods and tools that can determine subsystem power consumption with higher fidelity can be utilized [16], the current study adopts a first principles approach to keep computational time manageable. Interested readers may refer to previous work [10, 13] for a thorough explanation.

1) **Design requirements definition:** The point performance requirements and mission requirements (such as the cruise ceiling and Mach number, design mission payload and range) are defined in this module. As mentioned in Sec. II.A.1, only a Small Single-aisle Aircraft (SSA) with a conventional aft-tail, tube-and-wing, and an under-wing nacelle configuration is considered for this study.
2) **Aircraft & engine sizing:** This module parametrically defines the aircraft using top level geometric scales such as the wing reference area S_w, and propulsive scales such as rated thrust T_{SL}, and relevant weights such as the takeoff gross weight W_{TO} and the empty weight W_e. In the first iteration, an aircraft with a conventional subsystem architecture is sized as a starting point, since the FLOPS weight build-up equations are based on historical data of aircraft equipped with conventional subsystems. When the aircraft is re-sized in subsequent iterations, adjustment factors are used to modify component weights, fuel consumption, and drag polars to perform aircraft sizing with an unconventional subsystem architecture.
3) **Candidate subsystem architecture descriptor:** This module enumerates the architectures to be applied to the aircraft being sized (e.g. whether a particular subsystem is hydraulic, pneumatic or electric). The 13,824 architectures generated from the matrix of alternatives (Table 1) are represented in ISSAAC using the subsystem architecture descriptor introduced in Fig. 1.
4) **Subsystem architecture sizing and evaluation:** This module evaluates the weight, the time-varying bleed air and shaft-power requirement, and the time-varying direct drag increment of the subsystem architecture by sizing each major power consumer, distributor, and provider, and accumulating their individual effects.
5) **Mission performance impact evaluation and decomposition:** This module evaluates the impact on the mission performance due to changes in vehicle empty weight, secondary power requirements, and direct drag increment, which is transferred from the subsystem sizing modules in MATLAB to FLOPS through corresponding adjustment factors.
6) **Re-sizing of aircraft & subsystems:** In this module, an iterative process is carried out to re-size the aircraft and its subsystems in accordance with some re-sizing rules. The re-sizing process involves re-evaluation of the airframe, propulsion system, and subsystems in module 2, 4, and 5. The point performance capabilities and design mission requirements are held invariant, which leads to the requirement of a constant thrust-to-weight ratio (T_{SL}/W_{TO}) and wing loading (W_{TO}/S_w). Additionally, to ensure invariant stability and control characteristics, the stabilizer volume ratios are fixed at constant values.
7) **Post-processing analyses:** This is a customized module, which in this work includes determination of optimal subsystem architecture and optimal paths.

B. Verifying the Need for Optimal Paths

Table 1 shows the total number of alternatives with subsystem electrification options while keeping the design variables fixed. A full factorial design of experiment (DoE) was created to evaluate all possible electrified architectures. The current work focuses on two metrics of interest in the conceptual design phase – the Operating Empty Weight (OEW) and the Block Fuel Weight. Fixing the two objective metrics, the problem of populating the sets O_i ($i \in \{1, 2, \ldots, N\}$) can be tackled by a simple filtering algorithm to identify the non-dominated architectures constrained by the number of subsystem electrification changes allowed, where $N = 14$ is the total number of electrification changes possible.

Section II.B highlights the three hypotheses to be tested to establish the need for optimal paths in subsystem electrification. Evaluating a full factorial DoE of subsystem electrification options allows us to empirically verify all three hypotheses. Fig. 3 shows the full factorial architecture space that was evaluated for this purpose. It is interesting to note that the two big clusters that can be seen in Fig. 3 are caused by a single electrification change – ECS. To verify the first hypothesis, the sets of architectures in the constrained Pareto frontiers O_i ($i \in \{1, 2, \ldots, N-1\}$) are generated. The complete list of architectures that lie in the sets O_i is given in table 2, and these are also highlighted in Fig 3. One can see very clearly that the constrained Pareto optimal architectures are not the same as the unconstrained solutions, thus verifying hypothesis 1.

The second hypothesis can be verified if an architecture $\mathbf{A} \in O_N$ can be found not having one of its predecessor $\mathbf{A_p}$ in O_i ($i \in \{1, 2, \ldots, N-1\}$). From table 2, for *SSA-11110013300* $\in O_N$, one can see that *SSA-10000000000*, *SSA-10000001000*, *SSA-10000002000*, *SSA-10000003000* are all architectures which have number of changes equal to 1,

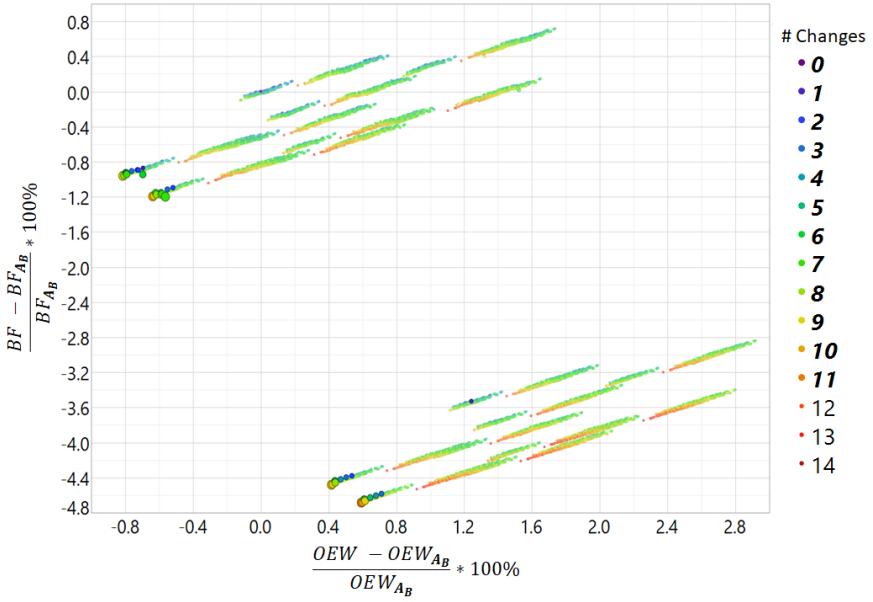

Fig. 3 Full factorial architecture solution space with A $\in O_i$ highlighted

2, 3, 4 respectively over the baseline, are predecessors of the chosen architecture, and yet do not lie in their corresponding constrained Pareto optimal sets O_i ($1 \leq i \leq 4$). Thus hypothesis 2 is verified. In fact, numerous such predecessor architectures can be generated as required. This means that while Eq. 1 depicts a valid path towards *SSA-11110013300*, it need not be better than one given by Eq. 2 since the intermediate architectures in the latter lie in the constrained Pareto optimal sets O_i.

$$\mathbf{A_B} \rightarrow \textit{SSA-10000000000} \rightarrow \textit{SSA-10000001000} \rightarrow \textit{SSA-10000002000} \rightarrow \ldots \rightarrow \textit{SSA-11110013300} \tag{1}$$

$$\mathbf{A_B} \rightarrow \textit{SSA-00000000300} \rightarrow \textit{SSA-01000000300} \rightarrow \textit{SSA-01010000300} \rightarrow \ldots \rightarrow \textit{SSA-11110013300} \tag{2}$$

To prove the the third hypothesis, at least one architecture $\mathbf{A} \in O_i$ must exist such that none of its successors are in O_N. Upon inspecting Table 2, it can be seen that *SSA-11001002300* $\in O_6, O_7$ does not have any successors in O_N. Thus, if decision makers with a budget of six subsystem electrification changes at once choose to go from the baseline to *SSA-11001002300*, they can find themselves having to undo the electrification of HLDA in order to reach the unconstrained optimal designs in the future. This verifies hypothesis 3 and proves that it is quite possible to get trapped in constrained locally optimal solutions with no path to the unconstrained optimal architectures without having to revert certain subsystem electrification changes. This then establishes the need for evaluating optimal paths to subsystem electrification. However, before proceeding, optimality criteria must be defined to establish a relative rank ordering of different paths to electrification.

C. Defining Path Optimality Criteria

Section III.B established the need to define optimal paths from the baseline to the architectures in the set O_N. While finding all possible paths in a directed acyclic graph **G** as defined in Sec. II.A.6 is computationally intractable for early aircraft design stages, finding the shortest path in **G** can be solved quickly using a variety of different shortest path algorithms in a scenario where paths have a single objective associated with them [17, 18]. When every path may have multiple independent objectives or weights, algorithms exist to tackle the multi-criteria shortest path problem [19–21]. However, the current paper faces unique difficulties in utilizing either of these approaches – First, the present work focuses on two objectives, the OEW and Block Fuel weight, and thus cannot directly utilize the single criterion shortest path algorithms. Second, weight vector associated with a path for the multi-criteria shortest path algorithms is given by Eq. 3. [19–21]

$$\begin{bmatrix} \Delta_{OEW_{path}} \\ \Delta_{BF_{path}} \end{bmatrix} = \begin{bmatrix} \Delta_{OEW_{edge1}} + \Delta_{OEW_{edge2}} & \ldots & +\Delta_{OEW_{edgeN}} \\ \Delta_{BF_{edge1}} + \Delta_{BF_{edge2}} & \ldots & +\Delta_{BF_{edgeN}} \end{bmatrix} \tag{3}$$

Table 2 Complete list of constrained Pareto optimal sets O_i with OEW and Block Fuel weight as objectives

O_i	Architecture Descriptors (SSA -)
O_1	*00000000300, 00000000001*
O_2	*01000000300, 00010000300, 00000000330, 00000000301*
O_3	*01000010300, 00010000330, 00010000301, 00000000331*
O_4	*01010010300, 01000010330, 01000010301, 00010000331*
O_5	*01110010300, 01010010330, 01010010301, 01000010331*
O_6	*01110010300, 11001002300, 01010010330, 01110010330 01110010301, 01010010331*
O_7	*01110010300, 11001002300, 01010013300, 01010010330, 01110010330, 11000012330, 01000013330, 01110010301, 01110010331*
O_8	*11010013300, 01010010330, 01110010330, 11000012330, 11010012330, 01010013330, 01110010301, 01010013301, 01110010331*
O_9	*11110013300, 11000012330, 11010013330, 11010013301 01110010331, 01010013331*
$O_{11} = O_{14} = O_N$	*11110013300, 11000012330, 11110013330, 11110013301, 11110013331*

Equation 3 works when path weights are defined uniquely for every edge of a graph. For this paper however, the starting node is fixed at $\mathbf{A_B}$, and every path from $\mathbf{A_B}$ to $\mathbf{A_t} \in O_N$ in $\mathbf{G}$ will have:

$$\Delta_{OEW_{path}} = \frac{(OEW_{\mathbf{A_B}} - OEW_{\mathbf{A_t}}) * 100\%}{OEW_{\mathbf{A_B}}} \tag{4}$$

$$\Delta_{BF_{path}} = \frac{(BF_{\mathbf{A_B}} - BF_{\mathbf{A_t}}) * 100\%}{BF_{\mathbf{A_B}}} \tag{5}$$

Traditional multi-criteria shortest path algorithms [19–21] will therefore not be able to distinguish between different paths based on a simple difference in OEW or BF metric as seen in Eq. 4 & Eq. 5. One way to solve this problem is to include metrics like the safety risks that will be unique for every intermediate architecture and can be estimated using methods given by Bendarkar et al. [22]. However, since this paper considers only OEW and Block Fuel as metrics of interest, the following cases are considered:

1. The multi-criteria case

As shown above, traditional implementations of multi-criteria shortest path solutions cannot be used for the problem at hand because every path ends up having the exact same objective vector for a given terminal architecture. One solution to this hurdle lies in utilizing the knowledge of the intermediate Pareto optimal sets O_i in defining path costs. One proposed solution is given by Eq. 6:

$$\begin{aligned} W_{jk} &= 1,\ \mathbf{A_k} \in O_i,\ i \in [1, 14] \\ &= 10,\ otherwise \\ W_{path} &= \sum_{\mathbf{A_B} \rightarrow \mathbf{A_t}} W_{jk} \end{aligned} \tag{6}$$

While it reduces the path finding problem to a single-criterion shortest path problem that can be easily tackled [17, 18], this approach utilizes the multi-objective optimization information obtained from the constrained Pareto fronts O_i. This approach will maximize the likelihood of intermediate architectures $\mathbf{A}$ belonging to O_i while traveling from $\mathbf{A_B} \rightarrow \mathbf{A_t}$.

2. The single-criterion case

The problem at hand involves minimizing both OEW and Block Fuel weight. To reduce it to a single criterion path minimization problem, a suitable single metric that can map the improvement in these two objectives needs to be defined. As explained above, a simple summation of improvement over baseline (Δ_{path}) for the two objectives will

results in all paths having the exact same weights for the same terminal architecture. Thus, the single metric needs to be defined so it can capture information provided by these deltas, while differentiating the different paths at the same time. The following different metrics are explored as possible solutions to the single criterion case:

The 2-Norm The 2-norm or the euclidean distance for the two objectives is given by Eq. 7, where the weight of edge connecting $\mathbf{A_i}$ to its successor $\mathbf{A_j}$ in $\mathbf{G}$ is given by W_{ij}.

$$\begin{aligned} W_{ij} &= (\Delta^2_{OEW_{ij}} + \Delta^2_{BF_{ij}})^{1/2} \\ \Delta_{OEW_{ij}} &= \frac{(OEW_{\mathbf{A_i}} - OEW_{\mathbf{A_j}}) * 100\%}{OEW_{\mathbf{A_B}}} \\ \Delta_{BF_{ij}} &= \frac{(BF_{\mathbf{A_i}} - BF_{\mathbf{A_j}}) * 100\%}{BF_{\mathbf{A_B}}} \\ W_{path} &= \sum_{\mathbf{A_B} \rightarrow \mathbf{A_t}} W_{ij} \end{aligned} \tag{7}$$

Since the euclidean distance of a path between two nodes is shortest for a straight line connecting the nodes, minimizing this weight ensures that the resultant shortest path in $\mathbf{G}$ is closest to the straight line connecting $\mathbf{A_B} \rightarrow \mathbf{A_t}$ in a two dimensional objective space of OEW and BF. Note that the improvement in the objectives is normalized by the baseline value to ensure both objectives are given equal preference.

The Inverse-Sum (I-S) This particular metric has been defined to ensure a path that provides similar overall improvements per subsystem electrification change gets higher preference (lower path weight) over a path that shows a huge improvement in one step, but lower improvements in other steps. Equations 8–12 provide the rational behind the path weight definitions provided in Eq. 11 . For any set of positive numbers, the AM-GM-HM inequality states that the arithmetic mean (AM) is greater than or equal to the harmonic mean (HM).

$$\begin{aligned} \frac{N}{\sum_{\mathbf{A_B} \rightarrow \mathbf{A_t}} \frac{1}{k + \Delta_{ij}}} &\leq \frac{\sum_{\mathbf{A_B} \rightarrow \mathbf{A_t}} k + \Delta_{ij}}{N} \\ k &= 1 + |\Delta_{path}| \end{aligned} \tag{8}$$

Equation 8 is a statement of the AM-GM-HM inequality, where Δ_{ij} is defined the same as in Eq. 7, k is heuristically defined to ensure $k + \Delta_{ij}$ – the variable of interest is always positive even if Δ_{ij} is negative, and N is the total number of edges in $\mathbf{A_B} \rightarrow \mathbf{A_t}$ (equal to total number of subsystem changes in $\mathbf{A_t}$). Inverting the inequality in the knowledge that $k + \Delta_{ij} > 0$ gives us Eq. 9

$$\sum_{\mathbf{A_B} \rightarrow \mathbf{A_t}} \frac{1}{k + \Delta_{ij}} \geq \frac{N^2}{\sum_{\mathbf{A_B} \rightarrow \mathbf{A_t}} k + \Delta_{ij}} \tag{9}$$

The inverse-sum metric can be defined as in Eq. 10, with the path weight given by Eq. 11. It can be seen from Eq. 11 that the path weight in this case is bounded on the lower side by a value that is inversely proportional to the arithmetic mean (AM) of $(k_{OEW} + \Delta_{OEW_{ij}} + k_{BF} + \Delta_{BF_{ij}})$.

$$W_{ij} = \frac{1}{k_{OEW} + \Delta_{OEW_{ij}} + k_{BF} + \Delta_{BF_{ij}}} \tag{10}$$

$$W_{path} = \sum_{\mathbf{A_B} \rightarrow \mathbf{A_t}} W_{ij} \geq \frac{N^2}{\sum_{\mathbf{A_B} \rightarrow \mathbf{A_t}} k_{OEW} + \Delta_{OEW_{ij}} + k_{BF} + \Delta_{BF_{ij}}} \tag{11}$$

The AM-GM-HM inequality also states that the three can only be equal when the individual values are all equal. The ideal minimum of W_{path} in Eq. 11 will occur if and only if all the edge improvements $((\Delta_{OEW_{ij}} + \Delta_{BF_{ij}})$ are equal to one another. As a consequence, minimizing the inverse-sum metric will ensure that every edge of the path leads to near equal improvement in $\Delta_{OEW} + \Delta_{BF}$ as given in Eq. 12.

$$min\ W_{path} \iff \Delta_{OEW_{ij}} + \Delta_{BF_{ij}} \approx \Delta_{OEW_{jk}} + \Delta_{BF_{jk}},\ \forall(\mathbf{A_i}, \mathbf{A_j}, \mathbf{A_k}) \in \mathbf{A_B} \rightarrow \mathbf{A_t} \tag{12}$$

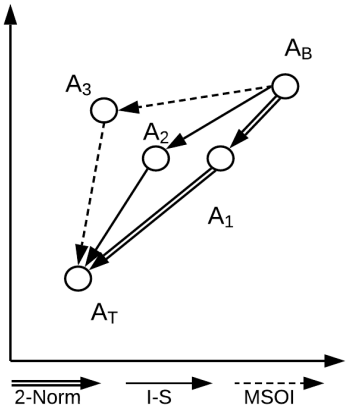

Fig. 4 Difference in path preference between the three single-criterion metrics

Greatest Single Objective Improvement (GSOI) The final metric considered for the single-criterion case involves weighting every edge in **G** by the greater percentage improvement between the two metrics of OEW and Block Fuel. The $\Delta_{OEW_{ij}}$ and $\Delta_{BF_{ij}}$ are defined the same as in Eq. 7. The edge weights in **G** in this case are defined as given in Eq. 13.

$$W_{ij} = k - max(\Delta_{OEW_{ij}}, \Delta_{BF_{ij}}) \tag{13}$$

$$W_{path} = \sum_{\mathbf{A_B} \rightarrow \mathbf{A_t}} W_{ij} \tag{14}$$

where $k = max(k_{OEW}, k_{BF})$ as given in Eq. 8. Minimizing this metric results in picking a path that seeks to maximize the improvement in single objective at every subsystem change level.

Figure 4 shows an example scenario where three possible paths are to be ranked based on the three single-criterion metrics discussed above. The 2-Norm metric prefers a path that is closest to the straight line joining $\mathbf{A_B}$ to $\mathbf{A_T}$, and thus chooses the path $\mathbf{A_B} \rightarrow \mathbf{A_1} \rightarrow \mathbf{A_T}$. The I-S metric prefers a path where every step yields equal new improvement in $\Delta_{OEW} + \Delta_{BF}$, and thus chooses the path $\mathbf{A_B} \rightarrow \mathbf{A_2} \rightarrow \mathbf{A_T}$. Finally, the GSOI metric seeks to maximize the benefit in either Δ_{OEW} or Δ_{BF} in every step, and thus chooses the path $\mathbf{A_B} \rightarrow \mathbf{A_3} \rightarrow \mathbf{A_T}$. Taken together, Sec. III.C.1 and III.C.2 provide four different methods to quantify the optimality of paths to subsystem electrification while being constrained by number of electrification changes allowed at a time. These sections seek to inform decision makers of possible metrics that can be utilized for this purpose in early aircraft design.

IV. Results

A. Optimal Paths from $\mathbf{A_B}$ to $\mathbf{A_T} \in O_N$

This section will examine the results of the methodology and single and multi-criteria path weighting approach that was developed in Sec. III. It is assumed that designers would want to achieve Pareto optimal architectures once the process of electrification is complete. Figure 5 shows the optimal paths to reach the set O_{14} as given in Table 2. Each row includes four sub-plots that show the paths from baseline to one of the architectures in O_{14} using the metrics defined in Sec. III.C. Placing plots for each edge weight criterion side-by-side enables easy comparison for the decision maker. On the vertical axis of each sub-plot, progressive electrification (top-to-bottom) in various subsystem components is shown. For example, the first four sub-figures show the optimal paths to reach architecture *SSA-11110013300* from the baseline using the 2-Norm, GSOI, I-S, and the multi-criteria metrics respectively as defined in Sec. III.C.

Consider the first (top-left) sub-plot within Fig. 5. This shows the optimal path obtained by minimizing the 2-norm metric while reaching *SSA-11110013300* from the baseline. Reading from the top to the bottom, we find that the WBS subsystem is electrified in the first step. This is followed by LGAS, THSA, TRAS, WIPS, PFCA (0->1), NWSS, PFCA (1->2->3) in that order to reach the terminal architecture of interest.

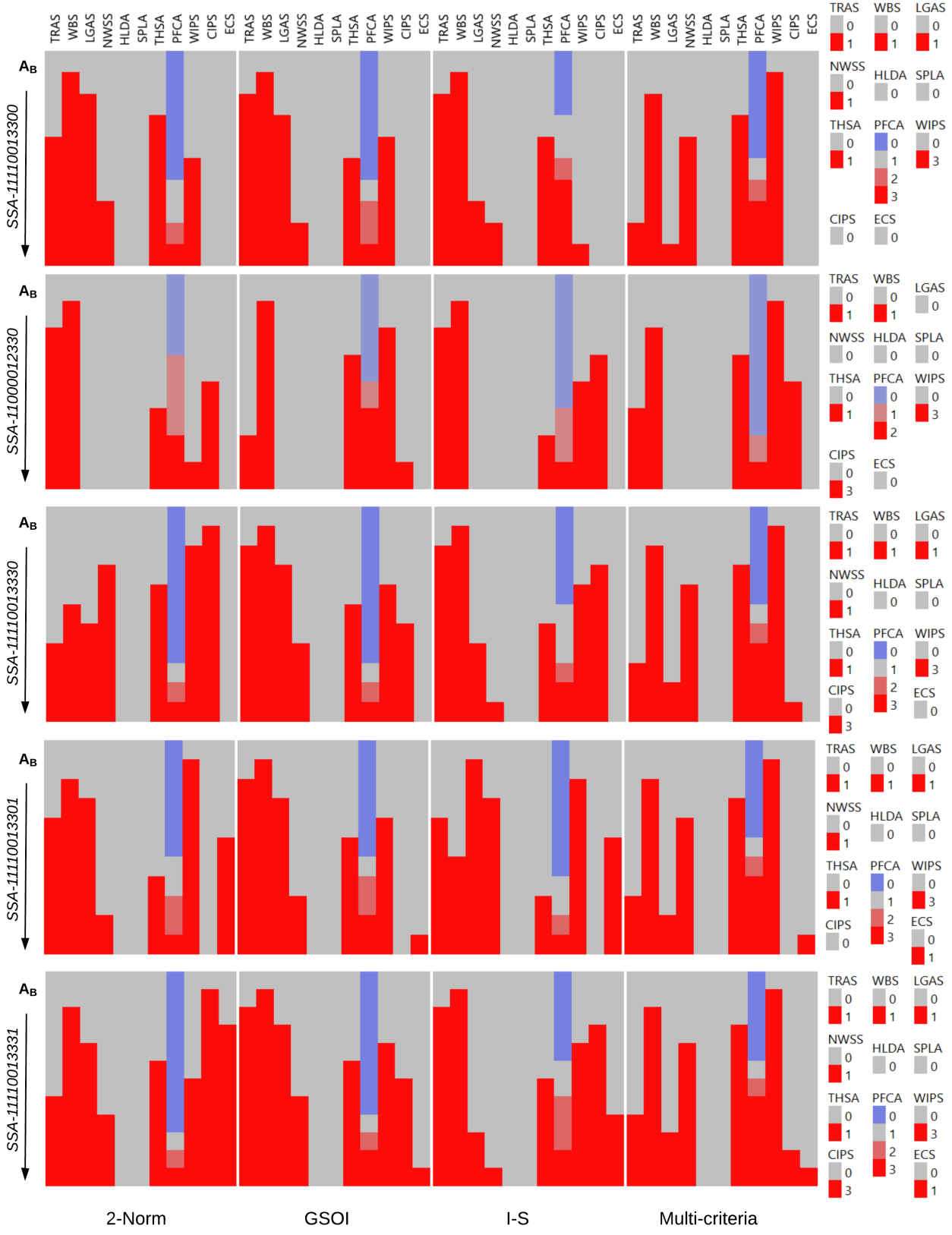

Fig. 5 **Optimal Paths to O_{14} with $\kappa_{spp} = 0$ (Refer Table 2)**

Figure 5 conveys information regarding the preferred sequence of subsystem electrification for every architecture in O_N, while simultaneously providing the reader with a top level overview of how the different optimal paths may suggest a possibly disparate choice of subsystem components to be electrified at each generational level. One can make the following observations quickly from Fig. 5:

1) The High Lift Device Actuation and Spoiler Actuation subsystems are rarely electrified in O_N.
2) Wheel Braking System and Wing Ice Protection System are among the first subsystems to be electrified irrespective of the optimality metric used.
3) It is preferable to electrify the Environmental Control System later rather than earlier in most of the optimal paths observed.
4) Once the gradual electrification of Primary Flight Control Actuators is started, it is preferable to complete the electrification of PFCA in consecutive changes (0->1->2->3).
5) Subsystems like the Nose Wheel Steering System, the Thrust Reverser Actuation System, the Cowl Ice Protection System, and the Primary Flight Control Actuators are always electrified somewhere in the middle of an optimal path leading from the baseline to O_N

It must be noted that the intent of this work is to enable the engineer to make such observations along with possible explanations for the observed behavior. These plots can be used to inform decision makers of a mathematically defensible set of results that can be utilized to determine an optimal sequence of changes to make while designing a More Electric Aircraft.

B. Effect of Modeling Uncertainty on Optimal Paths

The effect of modeling uncertainties in the decision making process for the presented method and sensitivity of the results is presented using the following assumption made in modeling the penalties arising due to electrification. This approach is identical to the one followed by Rajaram et al. [13]. Assumptions in the modeling of penalties in fuel flow due to extraction of shaft-power and bleed air (engine cycle parameters) to power the subsystems can have a significant effect on the Pareto-optimal solution set [13]. ISSAAC utilizes an approach based where the incremental fuel flow $\Delta\dot{w}_{f,spx}$ per engine due to total shaft-power extraction of P_{spx} is accounted for through the scalar k_p^* as

$$\Delta\dot{w}_{f,spx} = \dot{w}_{f,0}\, k_p^* \frac{P_{spx}[kW]}{N_{op,eng}\, T_{SL}[kN]}, \qquad \text{(per engine)} \tag{15}$$

where $\dot{w}_{f,0}$ is the conventional stock fuel flow rate for each of $N_{op,eng}$ engines assumed to contribute equally to the shaft-power P_{spx}. The incremental fuel flow $\Delta\dot{w}_{f,bx}$ due to bleed air extraction $\dot{w}_{bld} = \dot{m}_{bld} \cdot g$ is computed by employing the method of SAE AIR 1168/8 [23] to give

$$\Delta\dot{w}_{f,bx} = 0.0335 \left(\frac{T_{tet}[^\circ R]}{2000} \frac{\dot{w}_{bld}}{N_{op,eng}} \right), \qquad \text{(per engine)} \tag{16}$$

where T_{tet} is the turbine entry temperature, for which a representative value of 2,400°R is used in this work. Eq. 15 and Eq. 16 are useful as they require little information that is not already available in early aircraft design. At the same time, it is assumed they do not affect engine cycle parameters due to any sensitivities to secondary power extraction, and therefore do not require any redesign or resizing of the engines.

The uncertainty due to the aforementioned phenomenon on the design performance metrics of an electrified aircraft relative to a conventional one is quantified through κ_{spp}. This factor acts as a $k-$factor that alters the relationships shown above. For instance, particularly interesting cases are ones where either shaft-power extraction is *more* expensive than predicted by Eq. 15 and/or bleed extraction is *less* expensive than predicted by Eq. 16. These scenarios are accounted for by, (i) multiplying the RHS of Eq. 15 by the quantity $(1 + \kappa_{spp})$, and (ii) multiplying the RHS of Eq. 16 by the quantity $(1 - \kappa_{spp})$.

To assess the sensitivity of results (and hence the decision making process) to modeling uncertainties the experiment is repeated for two additional cases: (i) When shaft power extraction is 25% more expensive & bleed is 25% less expensive than predicted, and (ii) When bleed power extraction is 25% more expensive & shaft power is 25% less expensive than predicted. This amounts to evaluating two additional full factorial DoEs with 13824 cases each (see Table 1), with $\kappa_{spp} = \pm 0.25$. Figure 6 and Fig. 7 show the results for $\kappa_{spp} = \pm 0.25$ respectively, and are read in a similar manner as Fig. 5.

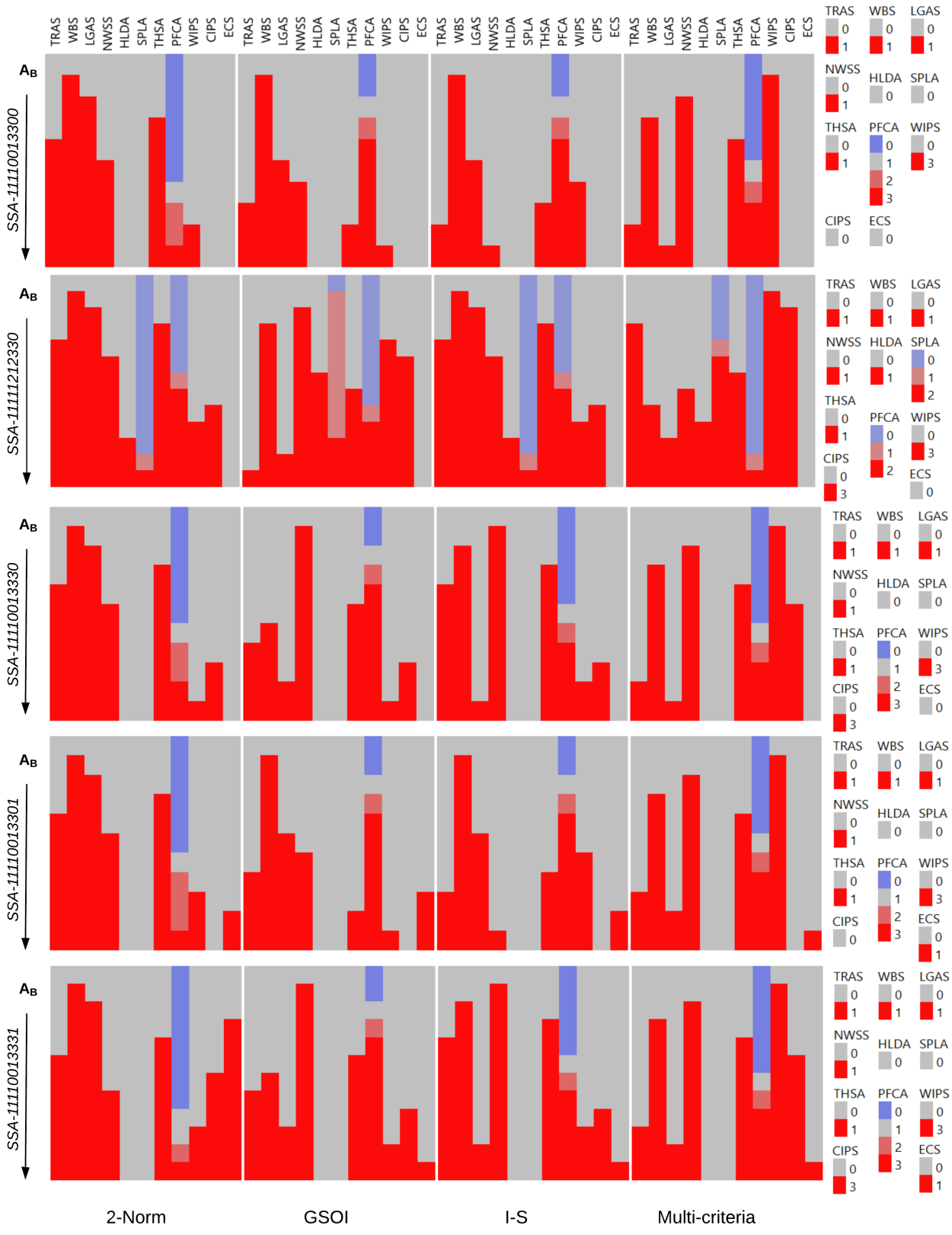

Fig. 6 Optimal Paths to O_{14} with $\kappa_{spp} = 0.25$

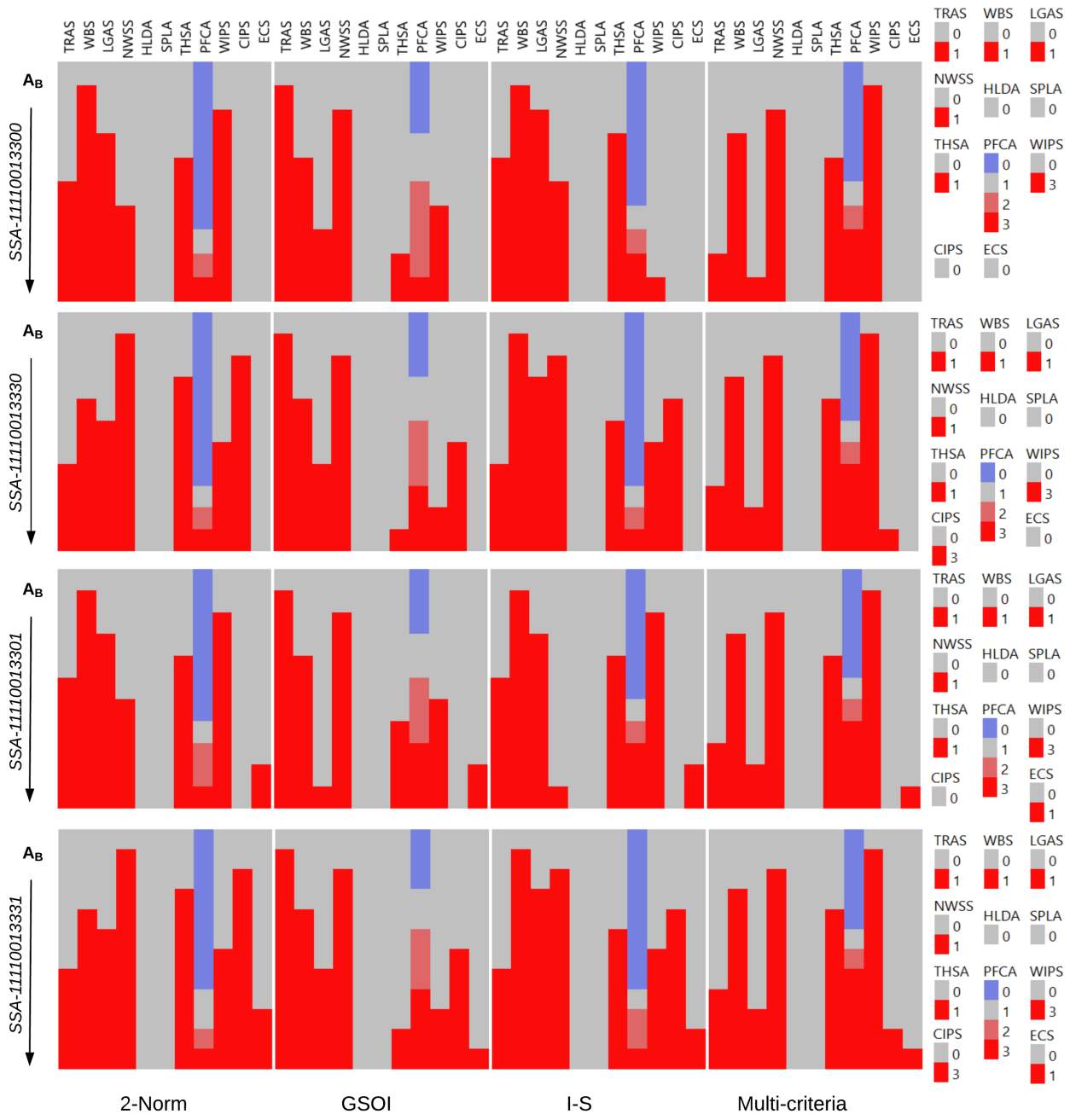

Fig. 7 Optimal Paths to O_{14} with $\kappa_{spp} = -0.25$

Figure 6 shows the optimal paths when shaft power is penalty is increased by 25%, while engine bleed is penalty is reduced by 25%. In this case, one can see that in general, the subsystem that depend on shaft power (e.g. TRAS, WBS etc.) are electrified earlier compared to subsystems that depend on bleed air (e.g. WIPS, CIPS). When bleed air penalty is increased by 25%, and shaft power penalty is reduced by 25%, the exact opposite can be observed. Fig. 7 shows that in general, the subsystems depending on bleed air now get electrified earlier compared to those that depend on shaft power. One can also observe that the architectures *SSA-11110013300*, *SSA-11110013330*, *SSA-11110013301*, and *SSA-11110013331* continue to lie in the unconstrained Pareto optimal set O_N even after the shaft and bleed penalties are changed, indicating that these architectures are robust to assumptions in modeling the impacts of subsystem electrification on aircraft OEW and Block Fuel.

V. Conclusions and Future Work

While the knowledge that MEA architectures are superior to conventional architectures is important, in practical scenarios it is insufficient. When multiple options exist in intermediate steps while undergoing a progression of changes, the question of which option to take while maintaining Pareto optimality and trade-off therein must be considered. This work developed and demonstrated a method to assess such situations and aid decision making. Subsystem electrification of an small single aisle aircraft using multi-criteria and single-criterion path optimality metrics was presented as a case study. It must be noted that while ISSAAC was utilized to generate results, the method itself is tool agnostic and can be utilized by decision makers to determine optimal paths when making discrete changes to a system architecture with a constraint on the number of allowable changes. Finally, additional results were generated to test the impact of uncertainty and assumptions in the modeling environment on the optimal paths generated. Future work can include the continuous system level variables in addition to the discrete architecture variables in the optimization problem to determine the interplay between simultaneously designing and electrifying subsystems under constraints on the number or allowable changes in the multi-objective setting. Additionally, system reliability metrics can be generated to allow the evaluation of truly multi-criteria Pareto-optimal paths.

Appendix

Table 3 Aircraft level design variables summary for Small Single-aisle Aircraft (SSA) Baseline

Aircraft data	**Aircraft Identification**
	SSA
Passenger capacity	170
Design range (NM)	3,000
Cruise Mach number	0.785
Max. ramp weight (lb)	175,130
Sea-level static thrust (lbf)	2 x 26,244
Wing planform area (ft^2)	1,347
Wingspan (ft)	114.8
Wing taper ratio	0.24
Wing 1/4-chord sweep (deg)	25
HT planform area (ft^2)	305
HT aspect ratio	5.47
HT taper ratio	0.37
HT 1/4-chord sweep (deg)	30
VT planform area (ft^2)	231
VT aspect ratio	1.80
VT taper ratio	0.30
VT 1/4-chord sweep (deg)	30
Fuselage length (ft)	123.3
Fuselage max. width (ft)	12.9
Fuselage max. height (ft)	12.9

References

[1] Raymer, D., *Aircraft Design: A Conceptual Approach*, 4^{th} ed., AIAA Education Series, 2006.

[2] Roskam, J., *Airplane Design Part V - Component Weight Estimation*, Design Analysis & Research, 1999.

[3] Torenbeek, E., *Synthesis of Subsonic Airplane Design: An Introduction to the Preliminary Design of Subsonic General Aviation and Transport Aircraft, with Emphasis on Layout, Aerodynamic Design, Propulsion and Performance*, Delft University Press, 1976.

[4] Jones, R., "The More Electric Aircraft: the past and the future?" *IEE Colloquium on Electrical Machines and Systems for the More Electric Aircraft*, 1999, pp. 1–4.

[5] Cronin, M., "The all-electric aircraft," *IEE Review*, Vol. 36, No. 8, 1990, pp. 309 –311.

[6] Chakraborty, I., and Mavris, D. N., "Integrated Assessment of Aircraft and Novel Subsystem Architectures in Early Design," *54th AIAA Aerospace Sciences Meeting*, 2016, p. 0215.

[7] Chakraborty, I., and Mavris, D. N., "Assessing Impact of Epistemic and Technological Uncertainty on Aircraft Subsystem Architectures," *16th AIAA Aviation Technology, Integration, and Operations Conference*, 2016, p. 3145.

[8] Lammering, T., "Integration of Aircraft Systems into Conceptual Design Synthesis," Ph.D. thesis, Institute of Aeronautics and Astronautics (ILR), RWTH Aachen University, 2014.

[9] Liscouet-Hanke, S., "A Model-Based Methodology for Integrated Preliminary Sizing and Analysis of Aircraft Power System Architectures," Ph.D. thesis, Universite' de Toulouse, 2008.

[10] Chakraborty, I., "Subsystem Architecture Sizing and Analysis for Aircraft Conceptual Design," Ph.D. thesis, Daniel F. Guggenheim School of Aerospace Engineering, Georgia Institute of Technology, Atlanta, GA, USA, December 2015.

[11] Cai, Y., Chakraborty, I., and Mavris, D. N., "Integrated Assessment of Vehicle-level Performance of Novel Aircraft Concepts and Subsystem Architectures in Early Design," *2018 AIAA Aerospace Sciences Meeting, AIAA Scitech Forum*, 2018. doi: 10.2514/6.2018-1741.

[12] Rajaram, D., Cai, Y., Puranik, T. G., Chakraborty, I., and Mavris, D. N., "Integrated Sizing and Multi-objective Optimization of Aircraft and Subsystem Architectures in Early Design," *17th AIAA Aviation Technology, Integration, and Operations Conference*, 2017, p. 3067.

[13] Rajaram, D., Cai, Y., Chakraborty, I., and Mavris, D. N., "Integrated Sizing and Optimization of Aircraft and Subsystem Architectures in Early Design," *Journal of Aircraft*, Vol. 55, No. 5, 2018, pp. 1942–1954.

[14] McCullers, L., *Flight Optimization System, Release 8.11, User's Guide*, NASA Langley Research Center, Hampton, VA 23681-0001, October 9 2009.

[15] Lytle, J. K., "The Numerical Propulsion System Simulation: An Overview," NASA/TM-2000-209915, `http://ntrs.nasa.gov/archive/nasa/casi.ntrs.nasa.gov/20000063377.pdf`, June 2000.

[16] Bendarkar, M. V., Chakraborty, I., Garcia, E., and Mavris, D. N., "Rapid Assessment of Power Requirements and Optimization of Thermal Ice Protection Systems," *AIAA Aviation Technology, Integration, and Operations Conference*, Atlanta, GA, 2018. doi:10.2514/6.2018-4136.

[17] Dijkstra, E. W., "A note on two problems in connexion with graphs," *Numerische Mathematik*, Vol. 1, 1959, pp. 269–271. doi:10.1007/BF01386390.

[18] Bellman, R., "On a routing problem," *Quarterly of Applied Mathematics*, Vol. 16, 1958, pp. 87–90. doi:10.1090/qam/102435.

[19] Martins, E. Q. V., "On a multicriteria shortest path problem," *European Journal of Operational Research*, Vol. 16, No. 2, 1984, pp. 236–245.

[20] Tung Tung, C., and Lin Chew, K., "A multicriteria Pareto-optimal path algorithm," *European Journal of Operational Research*, Vol. 62, No. 2, 1992, pp. 203–209. doi:10.1016/0377-2217(92)90248-8.

[21] Dell'Olmo, P., Gentili, M., and Scozzari, A., "On finding dissimilar Pareto-optimal paths," *European Journal of Operational Research*, Vol. 162, No. 1, 2005, pp. 70–82. doi:10.1016/j.ejor.2003.10.033.

[22] Bendarkar, M. V., Behere, A., Briceno, S., and Mavris, D. N., "A Bayesian Safety Assessment Methodology for Novel Aircraft Architectures and Technologies using Continuous FHA," *AIAA Aviation Forum*, Dallas, TX, 2019.

[23] *SAE AIR1168/8 - Aircraft Fuel Weight Penalty Due to Air Conditioning*, June 2004. doi:10.4271/AIR1168/8.